Author Manuscript
Author Manuscript
Author Manuscript
Author Manuscript

HHS Public Access
Author manuscript
Mol Cancer Ther. Author manuscript; available in PMC 2021 September 01.

Published in final edited form as:
Mol Cancer Ther. 2021 March ; 20(3): 577–588. doi:10.1158/1535-7163.MCT-20-0446.

Targeting radiation–resistant prostate cancer stem cells by B7-H3 CAR T cells

Yida Zhang[1,2], **Lile He**[1,#], **Ananthan Sadagopan**[1,#], **Tao Ma**[1], **Gianpietro Dotti**[3], **Yufeng Wang**[1], **Hui Zheng**[4], **Xin Gao**[5], **Dian Wang**[6], **Albert B. DeLeo**[1], **Song Fan**[1], **Ruochuan Sun**[1], **Ling Yu**[1], **Liyuan Zhang**[1], **Gongxian Wang**[2], **Soldano Ferrone**[1,7], **Xinhui Wang**[1,*]

[1]Division of Surgical Oncology, Department of Surgery, Massachusetts General Hospital, Harvard Medical School, Boston, MA, USA

[2]Department of Urology, The First Affiliated Hospital of Nanchang University, Nanchang, Jiangxi, China

[3]Lineberger Comprehensive Cancer Center and Department of Microbiology and Immunology, University of North Carolina, Chapel Hill, NC, USA

[4]Biostatistics Center, Massachusetts General Hospital, Harvard Medical School, Boston, MA, USA

[5]Division of Hematology/Oncology, Department of Medicine, Massachusetts General Hospital, Harvard Medical School, Boston, MA, USA

[6]Department of Radiation Oncology, Rush University Medical Center, Chicago, IL, USA

[7]Department of Orthopaedic Surgery, Massachusetts General Hospital, Harvard Medical School, Boston, MA, USA

Abstract

Radiation therapy (RT) is a key treatment for prostate cancer (PCa). However, RT resistance can contribute to treatment failure. PCa stem cells (PCSCs) are radioresistant. We recently found that fractionated irradiation (FIR) preferentially upregulates expression of the immune checkpoint B7-H3 (CD276) on PCSCs compared to bulk cells in each PCa cell line tested. These findings prompted us to investigate whether B7-H3 CAR T cells, which may abrogate function of an immune checkpoint and mediate lysis of targeted cells, can target RT-resistant PCSCs *in vitro* and *in vivo.* B7-H3 expression is naturally higher on PCSCs than bulk PCa cells and cytotoxicity of B7-H3 CAR T cells to PCSCs is more potent than to bulk PCa cells. Furthermore, FIR preferentially and significantly upregulates B7-H3 expression on PCSCs and bulk PCa cells. The duration of FIR or single-dose irradiation-induced upregulation of B7-H3 on PCa cells and PCSCs lasts for up to 3 days. B7-H3 CAR T cell cytotoxicity against FIR-resistant PCSCs at a low effector to target ratio of 1:1 was assessed by flow analysis and sphere formation assays.

[*]**Corresponding author:** Xinhui Wang, MD, PhD, Division of Surgical Oncology, Department of Surgery, Massachusetts General Hospital, Harvard Medical School, Phone: 617-726-7881, Fax: 617-726-8623, xwang30@mgh.harvard.edu.
[#]These authors have contributed equally to this work.

Conflicts of Interest:
The authors declare no potential conflicts of interest.

Author Manuscript Author Manuscript Author Manuscript Author Manuscript

Upregulation of B7-H3 expression by FIR made PCSCs even more sensitive to B7-H3 CAR T cell-mediated killing. Consequently, the FIR and B7-H3 CAR T cell therapy combination is much more effective than FIR or CAR T cells alone in growth inhibition of hormone insensitive PCa xenografts in immunodeficient mice. Our work provides a sound basis for further development of this unique combinatorial model of RT and B7-H3 CAR T cell therapy for PCa.

Significance: We demonstrate that FIR preferentially upregulates B7-H3 expression by RT-resistant PCSCs vs. bulk cells; cytotoxicity of B7-H3 CAR T cells on FIR-treated PCSCs is potent and results in significantly improved anti-tumor efficacy in mice.

Keywords

B7-H3 CAR T cells; Prostate cancer; Prostate cancer stem cells; fractionated irradiation (FIR); Radiation-resistant

INTRODUCTION

Prostate cancer (PCa) is the most common non-cutaneous cancer among American men with an estimated 191,930 new cases in 2020 and the third highest cause of cancer deaths in the U.S., with an estimated 33,330 deaths (1). Organ-confined PCa is typically treated with surgery and/or radiation therapy (RT), the latter given as brachytherapy or external beam RT (2). Specifically, RT alone or RT in combination with androgen deprivation therapy is commonly recommended to treat post-prostatectomy patients with high-risk features such as extracapsular extensions, positive surgical margins, or persistent/rising prostate-specific antigen levels, as well as newly diagnosed patients with low-volume metastatic disease (3). However, RT is associated with a biochemical recurrence rate of 20-30% in patients with organ-confined PCa and is unlikely to be curative for patients with locally advanced disease or multiple high-risk features post-prostatectomy (4,5). Resistance to RT contributes to PCa recurrence and mortality (6) and subclinical micrometastases present at diagnosis contribute to early biochemical failure and distant metastasis (7). This clinical challenge underscores the urgency to develop therapies more effective than those currently available for PCa patients.

Considerable evidence indicates that cancer treatment resistance and recurrence is due to cancer stem cells (CSCs), a small subpopulation of tumor cells present in the bulk tumor and/or metastases, which have “stem cell-like” properties, including chemo- and radio-resistance (8,9). These CSCs have been identified and isolated from a wide range of human tumors, including PCa (8–12). Like other human CSCs studied, human prostate CSCs (PCSCs) have been shown in animal tumor model systems to have high tumorigenicity in immunodeficient mice and metastatic potential (10).

Cancer immunotherapy has been successfully applied clinically to a number of cancer types, including PCa. The dendritic cell vaccine therapy sipuleucel-T has been approved since 2010 for treatment of patients with metastatic castration-resistant PCa (13), and ongoing clinical trials are evaluating additional immunotherapies, such as immune checkpoint inhibitors and adoptive cell therapies (14). Indeed, all elements of the host’s immune system are now being clinically employed in various forms of passive and active immunotherapeutic

Author Manuscript Author Manuscript Author Manuscript Author Manuscript

protocols. One of the most innovative approaches combines antibody fragments with T cell-based immunology to target cancer cells, namely, the development of genetically engineered chimeric antigen receptor (CAR) T cells (15). By combining the tumor antigen (TA) epitope recognition of an antibody fragment with the properties of a T cell receptor, the CAR T cell has the potential to recognize tumor-associated/specific molecules presented on the tumor cell surface and induce the cytolytic activity of a T cell to mediate tumor cell lysis.

To date, however, CAR T cell therapy has demonstrated enhanced anti-tumor activity against blood cancers compared to solid tumors (16). Although anti-CD19 and anti-CD22 CAR T cell therapy for leukemia have been successful overall, treatment failures due to low levels of antigen expression as well as immunoselection of epitope loss variants are common (17,18). In addition, the challenges for successful application of CAR T cell therapy for solid tumors include the increased heterogeneity of solid tumors relative to leukemias, identifying suitable high-density antigenic targets, and migration of anti-tumor T cells, especially adoptively transferred immune effector cells, into the hostile tumor microenvironment, which can reduce their persistence and functionality.

Currently, three tumor-associated antigens have been targeted in clinical trials of CAR T cell therapy for metastatic PCa patients. In general, patients in these trials have not responded beneficially to any significant degree to CAR T cell therapy against the prostate-specific membrane antigen (PSMA) and prostate stem cell antigen (PSCA) (19). Clinical trials targeting the third TA, the epithelial cell adhesion molecule (EpCAM), with CAR T cells are currently being conducted and evaluated for several cancers, including PCa (19). However, as noted above, one challenge in making a CAR T-cell therapy effective for PCa is the choice of the targeted TA. For instance, PSCA is not expressed on all PCa (20) and PSMA is expressed in brain tissue, which raises the possibility of serious therapy complications (21). Further understanding and selection of new PCa TAs has significant potential to strengthen the effectiveness of CAR T cell-based PCa therapy.

In recent years, the development of various classes of agents having the ability to upregulate T cell-based anti-tumor immune response by blocking immune checkpoints has greatly contributed to the increased clinical application of tumor immunotherapy (22). Tumor cells express immune checkpoints, which interact with cytotoxic T lymphocytes (CTL) and block the ability of these effectors to mediate cytolysis of the targeted tumor cells. B7-H3 is an immune inhibitory molecule expressed at elevated levels in a large number of cancer types, including pancreatic ductal adenocarcinoma (PDAC), ovarian cancer (OC), lung cancer, clear cell renal carcinoma and PCa (15,23). In PCa, elevated expression level of B7-H3 is associated with high Gleason score, advanced stage, metastases, and poor patient prognosis (23,24). Clinical targeting of B7-H3 with the monoclonal antibody (mAb) enoblituzumab has resulted in tumor regression in patients with treatment-refractory PCa (25). Recent studies have found strong evidence that B7-H3 regulates T-cell-mediated immune response and inhibition of B7-H3 results in T-cell proliferation (26,27). Moreover, blocking activated T cells with a bispecific anti-CD3x anti-B7-H3 antibody enhanced T cell cytotoxicity and increased cytokine production of IFNγ, TNFα, and IL-2 (28). Crucially, B7-H3 expression is minimal in healthy tissue (26).

Author Manuscript Author Manuscript Author Manuscript Author Manuscript

The present study focuses on the development of a CAR T cell therapy targeting the immune checkpoint B7-H3, which is expressed on PCSCs and bulk PCa cells. The B7-H3 CAR T cells used in this study are expected to be bifunctional; they can abrogate the B7-H3 immune checkpoint and mediate lysis of targeted tumor cells. The anti-B7-H3 CAR construct was derived from the single-chain variable fragment (scFv) of the B7-H3-specific 376.96 mAb (15) and already has demonstrated significant and persistent cytolytic activity against PDAC, OC, and neuroblastoma in previous studies (15).

Combinatorial approaches have led to multiple recent successes in the treatment of advanced PCa and other cancers (29–31). The aims of this study were to evaluate the efficacy of B7-H3 CAR T cell therapy against RT-resistant PCa. The CAR T cells were used as a monotherapy or in combination with FIR against two human PCa cell lines, DU145 and PC3, in *in vitro* and *in vivo*-based preclinical experiments with particular emphasis on evaluating the targeting of FIR-resistant PCSCs, which are responsible for tumor formation, progression and metastasis and thus may be responsible for treatment failure and mortality (10–12).

MATERIALS AND METHODS

Cell lines and cell culture.

The human PCa cell lines DU145 and PC3, and the human Burkitt's lymphoma Raji cell line were purchased from the American Type Culture Collection (ATCC). The human breast cancer SUM159 cell line was obtained from Asterand Bioscience Inc (Detroit, MI) and the SUM159 B7-H3 knockout (KO) cell line was generated by CRISPR-Cas9 knockout kit (Cat# sc-402032, Santa Cruz Biotechnology, Dallas, TX) in our laboratory. All the cell lines were cultured in RPMI 1640 medium (Corning Incorporated, Corning, NY) supplemented with 2 mmol/L L-glutamine (Corning) and 10% fetal bovine serum (FBS; Gemini Bio-Products LLC, West Sacramento, CA) at 37°C in a 5% CO2 humidified atmosphere.

Animals.

Eight-week-old, male NSG mice were obtained from the Massachusetts General Hospital COX7 animal facility. The Institutional Animal Care and Use Committee has approved all the animal studies.

FIR or single-dose IR.

In vitro, cells plated in 6-well plates (Corning) at a density of 5×10^5 cells/well in 2 mL RPMI 1640 medium containing 10% FBS were irradiated with a single dose of IR (0, 2, 6, 10, 16 or 20 Gray [Gy]) or FIR (2 Gy daily for 3 or 5 days). *In vivo,* FIR at 4Gy/daily was delivered locally at the indicated fractions to each mouse tumor area while the remaining body was covered by a lead shield. The X-RAD 320 Biological Irradiator (Precision X-ray Inc., CT) was used for all *in vitro* and *in vivo* experiments.

Identification of $ALDH^+CD44^+$ PCSCs.

Tumor cells were stained using the ALDEFLUOR (Stem Cell Technologies, CT) and anti-human CD44 (clone#G44-26, Miltenyi Biotec Inc., CA). The $ALDH^+CD44^+$ PCSCs were

Author Manuscript Author Manuscript Author Manuscript Author Manuscript

detected by flow cytometry using a BD Accuri C6 flow cytometer (BD Biosciences, CA) and sorted using a FACS Aria II Cell Sorter Flow Cytometer (BD Biosciences) (32).

Generation of B7-H3 CAR T cells.

Peripheral blood mononuclear cells (PBMCs) were isolated from normal human donor blood (Research Blood Components, MA) with Lymphoprep (Stem cell Technologies). On day 0, the PBMCs (1×10^6/well) were activated in a non-treated 24-well cell culture plate (#351147,Corning) pre-coated with 1 μg/mL CD3 (clone OKT3, Miltenyi Biotec) and 3 μg/mL CD28 antibodies (clone CD28.2, BD Biosciences) in the complete medium (45% RPMI1640 and 45% Click's medium [Irvine Scientific, CA], 10% FBS, 1% Penicillin and 1% Streptomycin [Corning]). On day 1, activated T cells were expanded by addition of IL-7 (10 ng/mL, PeproTech, NJ) and IL-15 (5 ng/mL, PeproTech) (CAR T medium). On day 2, the activated and expanded T cells were transferred to wells of 24-well plates that had been previously coated with RetroNectin (Takara Bio Inc., Shiga, Japan) and contained retroviral particles of the B7-H3 CAR construct (15). On day 4, to allow for their continued expansion, the transduced cells were collected and transferred to tissue culture-treated 24-well plates (Cat#353047 Corning) with each well containing 0.5 mL of the activated T cell suspension (5×10^5 cells/well) and 1.5 mL of fresh CAR T medium. On day 6, an aliquot of transduced cells was analyzed for transduction efficiency and 50% CAR T spent medium was replaced with fresh medium, i.e., 50:50 (v./v.) old medium: new medium. On day 8, CAR T cells were counted and reseeded at 1×10^6/well in 2mL of fresh CAR T medium to further expand cells. On day 10, 50% spent medium was replaced with the fresh medium as done on day 6. On day 12-13, CAR T cells and non-transduced T (NT) cells grown at similar conditions were collected, aliquoted, and frozen for storage in a liquid nitrogen freezer for *in vitro* and *in vivo* experiments.

Flow cytometry analysis.

PC3, DU145, Raji, and SUM159 B7-H3 KO cells (10^7 cells) were stained with the human B7-H3 specific mouse mAb 376.96 (1 μg/ml) for 30 min at 4°C and washed twice with 0.5% BSA/PBS using mouse mAb F3C25 as isotype control (33). Cells were then stained with R-Phycoerythrin AffiniPure F(ab')$_2$ Fragment Goat Anti-Mouse IgG (H+L) (Jackson ImmunoResearch Inc., PA) (1:100) as the secondary antibody for 30 min at 4^0C and washed twice with 0.5% BSA/PBS. Cell surface expression of the scFv of mAb 376.96 on CAR T cells was determined by incubating the cells with 10% human AB serum/PBS (Cat# HP1022HI, Valley Biomedical Products and Services Inc., Winchester, VA) for 15 min, followed by two washes with 0.5% BSA/PBS and staining with recombinant human B7-H3 Fc Chimera Protein, CF (R&D Systems, MN) and then R-Phycoerythrin AffiniPure F(ab')$_2$ Fragment Goat Anti-Human IgG, Fcγ fragment specific antibodies (Jackson ImmunoResearch) and APC-Cy™7 Mouse Anti-Human CD3 mAb (Clone SK7, BD Biosciences). The phenotype of CAR T cell-surface antigens was determined by staining the cells with PE/Cyanine7 anti-human CD3 (clone UCHT1), FITC anti-human CD4 (clone A161A1), APC/Cyanine7 anti-human CD8 (clone SK1), APC anti-human CD45RA (clone HI100), and PE anti-human CD62L (clone DREG-56) antibodies. All these reagents were purchased from Biolegend Inc., San Diego, CA and the cells analyzed by flow cytometry using the LSR II cytometer (BD Biosciences) and FlowJo software.

Author Manuscript Author Manuscript Author Manuscript Author Manuscript

Clonogenic assay.

DU145 and PC3 PCa cells were seeded into 6-well plates at a density of 5×10^5 cells/well and cultured overnight at 37°C in a 5% CO_2 humidified atmosphere. Cells were irradiated with 2Gy for either 3 or 5 days and incubated for 10-14 days under previously described conditions. Colonies comprised of 50 cells or more were counted as described (8).

Apoptosis assay.

Apoptotic cells were detected using FITC Annexin V Apoptosis Detection Kit with 7-AAD (Biolegend). FIR-treated cells were collected, washed, resuspended at a cell density of 10^6 cells/500 μL of 1X binding buffer, and stained with 5 μL of annexin V-FITC and 5 μL of 7AAD at RT for 15 min in the dark. A minimum of 10,000 cells within the properly gated region were analyzed for apoptosis by flow cytometry (32).

Sphere formation assay.

Non-necrotic tumor tissue specimens harvested from xenograft-bearing NSG mice were collected at the time of sacrifice and a single cell suspension was obtained as previously described (9). Cultured tumor cells treated with FIR or co-cultured with CAR T cells, or single cell suspensions of xenograft tumors were seeded (300 cells/well) in triplicate wells in 24-well ultra-low attachment plates (Corning) in sphere formation medium as previously described (9).

In vitro cell cytotoxicity assays.

Target cells (5000 cells/well) were plated in 96-well plates (Cat#:353072, Corning) in 100 μL of complete growth medium and grown overnight. B7-H3 CAR T cells were added to the wells the next day at the indicated effector to target (E:T) ratios and cultured for 48 hrs at 37 ^{0}C in a 5% $_{CO2}$ humidified atmosphere. T cells were removed by washing with PBS. The targeted tumor cells were quantified by a viable cell MTT assay, as described (34) or co-cultured cells were simultaneously stained for residual tumor cells by B7-H3 specific mouse mAb 376.96 and R-Phycoerythrin AffiniPure F(ab')$_2$ Fragment Goat Anti-Mouse IgG (H +L) and CAR T cells by APC-Cy™7 Mouse Anti-Human CD3 and analyzed by a flow cytometer.

In vivo prostate xenograft models.

DU145 cells (2×10^6 cells/mouse) or PC3 cells (5×10^6 cells in 50 μL RPMI 1640 serum-free medium mixed with 50 μL Matrigel [Corning]/mouse) were implanted subcutaneously using a 22-gauge needle (BD Biosciences) in the right thighs of NSG mice. Body weight and tumor volume were measured every 3 days. Treatments were initiated when the tumors had an approximate diameter of 50 mm^3. Mice were divided into n=4 (DU145 model) or n=5 (PC3 model) groups using a stratified randomization strategy (n=5 mice/group), such that the difference of mean tumor volumes was not statistically significant between each group. FIR (4Gy/day) was delivered to local tumor area at indicated times. A single treatment with B7-H3 CAR T cells or NT cells (10^6 cells/mouse) was given through tail-vein injection at different specified times. Mice were left untreated as controls. Tumor volumes were measured by digital caliper and calculated by the formula: volume = 1/2 x length x $width^2$.

Author Manuscript Author Manuscript Author Manuscript Author Manuscript

The dose of FIR was chosen because it is between clinical moderate hypofractionation (2.4-3.4 Gy/fraction) and ultrahypofractionation (≥5Gy/fraction) (35).

Immunofluorescence staining of frozen PCa xenograft tissue sections.

Optimal cutting temperature compound (OCT)-embedded frozen xenograft tissue blocks were sectioned by a microtome-cryostat into 4-5 μm thick tissue slides. These tissue slides were stained by primary mAb 376.96 (0.1 μg/mL) and detected with the Goat Anti-Mouse IgG (H+L) Highly Cross-Adsorbed Secondary Antibody, Alexa Fluor Plus 594 (diluted at 1:500) (Catalog #A32742, Thermo Fisher). Cell nuclei were counterstained with DAPI.

Statistical methods.

A two-tailed Student's *t* test or a one-way ANOVA with Tukey HSD post-hoc tests were performed to interpret the differences between experimental and control groups. All *in-vitro* experiments were conducted three times. Differences between B7-H3 CAR T cell-mediated cytotoxicity on different cell populations (including all three E:T ratios) was detected using a chi-square test in a two-way ANOVA. Differences between tumor volumes were analyzed by chi-square test in an ANOVA with repeated measurements. The above models were fitted using SAS version 9.4 (SAS Institute, Inc., Cary, NC).

RESULTS

PCSCs are resistant to FIR.

It has been known that PCSCs are resistant to irradiation (IR) (36,37). Moreover, IR induces PCSCs (38). In agreement with the literature, it was determined that PCSCs, defined as $ALDH^{+}CD44^{+}$ cells (39), were enriched from 0.35±0.18% to 15.67±3.51% (p<0.01) and from 0.43±0.12% to 11.2±2.95% (p<0.01) in DU145 and PC3 cell lines, respectively, in response to a clinically relevant FIR setting (2Gy/day x 5 days). In both cell lines, the enrichment of PCSCs was proportional to the total FIR dose (Fig 1A–C). In addition, sphere formation, a common *in vitro* functional marker for identifying CSCs, confirmed the results of the flow cytometry analysis and showed the FIR-resistance of PCSCs. FIR treatment (2Gy/day x 5 days) increased sphere formation 2.5-fold (p<0.05) and 3.3-fold (p<0.05) in DU145 and PC3 cells, respectively, compared to untreated cells (Fig 1D–F). Relative to untreated cells, FIR induced significantly more apoptotic cells in the bulk cell populations of DU145 (29.87±3.35% vs. 2.37±0.55%) (p<0.001) and PC3 (19.8±2.4% vs. 2.73±0.68%) (p<0.001) cell lines, respectively. Induction of apoptosis was dose-dependent. FIR of 2Gy/day x 3 days induced lower levels of apoptosis than FIR of 2Gy/day x 5 days in DU145 (17.7±1.66% vs 29.87±3.35%) (p<0.01) and PC3 (12.3±1.51% vs 19.8±2.4%) (p<0.05) cells (Fig 2A–C). Similarly, FIR significantly reduced, but did not eradicate cells in a clonogenic assay, which tested at the single cell level its long-term effects on colony formation of DU145 and PC3 cells (Fig 2D–G).

PCSCs express higher levels of B7-H3 antigen than bulk PCa cells.

In general, CAR T cell therapy is antigen-specific, and its efficacy is dependent on the level of expression of the targeted antigen on the tumor cell (17). Recently, we developed an effective therapeutic strategy for PDAC using CAR T cells that target B7-H3 (15). As the

Author Manuscript Author Manuscript Author Manuscript Author Manuscript

first step in applying this strategy to PCa, the level of B7-H3 expression on PCSCs in the PCa cell lines was studied. Although 100% of PCSCs and bulk tumor populations expressed B7-H3, its expression on PCSCs was found to be significantly higher in both cell lines, as measured by mean fluorescence intensity (MFI) (2.4-fold higher in DU145 cells (p<0.001) and 2.2-fold higher in PC3 cells (p<0.001)) (Fig 3A–D). The flow data are specific, as SUM159 B7-H3 KO cells and Raji cells, which do not express endogenous B7-H3, served as controls and stained negative (Fig 3E, F).

FIR enhances B7-H3 expression on PCSCs and bulk PCa cells.

For a rational basis in designing a combinational approach using FIR and B7-H3 CAR T cells to treat PCa, the impact of FIR on B7-H3 expression by PCSCs and bulk PCa cell populations in DU145 and PC3 cells was investigated by flow analysis with B7-H3-specific mAb 376.96 (Supplementary Fig 1A, B). In both PCa cell lines tested, FIR (both doses) significantly increased B7-H3 expression levels on PCSCs and bulk PCa cell populations compared to untreated cells, as determined by MFI (p<0.05). The total FIR dose, however, did not seem to make a significant difference on B7-H3 expression of either cell population. Moreover, regardless of treatment, PCSCs expressed significantly more B7-H3 than bulk cells (p<0.001) (Fig 4A, B). Additionally, a single dose of IR increased B7-H3 expression on both PCSCs and bulk cells in a dose-dependent manner up to 10Gy, with significant B7-H3 upregulation observed at 6Gy (p < 0.05), 10Gy (p < 0.01), 16Gy (p < 0.01), and 20Gy (p < 0.01). However, a single dose of >10Gy IR (16Gy or 20Gy) did not further increase B7-H3 expression on either bulk cells (Fig 4C, D) or PCSCs (Fig 4E, F) (Supplementary Fig 2A, B). 10Gy single dose IR-induced B7-H3 upregulation on bulk cells was also time-dependent, with B7-H3 expression greater on day 3 vs. day 1 post-IR (p<0.05) in DU145 cells and a trend towards this in PC3 cells. However, B7-H3 expression started to drop by day 5 post-IR and by day 7, the levels of B7-H3 were not significantly different from untreated cells (p>0.05) (Fig 4G, H). In contrast, 10Gy single dose IR-induced B7-H3 upregulation on PCSCs lasted from days 1-5 post-IR without much change. By day 7 post-IR, the levels of B7-H3 were not significantly different from untreated cells (p>0.05) (Fig 4I, J, Supplementary Fig 2C, D).

Generation and phenotype of B7-H3 CAR T cells.

To generate B7-H3 CAR T cells for use in therapy of PCa, the mAb 376.96 scFv used to determine B7-H3 expression by PCa was selected as the CAR of the retroviral construct. It was linked with a CD8α hinge and transmembrane domain, followed by a CD28 costimulatory domain coupled to a CD3ζ intracellular signaling domain (Fig 5A) (15). PBMCs isolated from three healthy donors were cultured in the presence or absence of retroviral construct supernatants and used to generate B7-H3 CAR T cells and NT cells, respectively. Both populations expanded equally over time (Fig 5B). After 8 days of culture, 64±4.36% of the transduced CAR T cells derived from PBMCs obtained from the three donors were B7-H3^{+} (Fig 5C), while NT cells were negative for surface expression of the B7-H3-specific scFv 376.96 by flow cytometry. After 11 days of culture, the number of B7-H3 CAR T cells and NT cells both increased more than 10-fold (Fig 5B), but NT cells continued to show non-detectable levels of 376.96 scFv expression. The B7-H3 CAR T cells and NT cells showed a similar percentage of CD4^{+} (33.33±2.08% vs. 37.33±3.06%;

Author Manuscript Author Manuscript Author Manuscript Author Manuscript

p=0.1342) and $CD8^+$ T cells (64.67±2.08% vs. 60.67±3.06%; p=0.1342), as well as a similar percentage of memory $CD45RA^+CD62L^+$ T cells (61.33±3.51% vs. 57.67±5.13%; p=0.3648) (Fig 5D–G).

PCSCs are more sensitive to B7-H3 CAR T cells than bulk PCa cells *in vitro*.

To assess whether the B7-H3 CAR T cells were able to mediate cytolysis of PCSCs, sorted $ALDH^+CD44^+$ PCSCs cells and bulk PCa cells were co-cultured with B7-H3 CAR T cells at different E:T ratios for 48hrs. As measured by MTT assays, cytolysis of both cell populations by B7-H3 CAR T cells in each cell line tested was dose and antigen expression level-dependent. At E:T ratio of 5:1, >95% of PCSCs and bulk PCa cells were killed, whereas at E:T ratio of 1:1, 63.41±3.32% PCSCs and 30.82±4.67% bulk cells of the DU145 cell line (p<0.001), as well as 66.90±0.19% PCSCs and 30.22±3.40% bulk cells of the PC3 cell line (p<0.001) were eliminated. In contrast, at E:T ratio of 1:5, there was almost no killing of either target cell population. Importantly, analysis of the two whole curves (all three E:T: ratios) confirmed that B7-H3 CAR T cell-mediated cytotoxicity is greater on PCSCs than on bulk cells in cell lines DU145 (p<0.001) and PC3 (p<0.001) (Fig 6A, B). The cytolysis was antigen-specific, as use of NT effectors or SUM159 B7-H3 KO cells as targets resulted in no measurable cytotoxicity (Fig 6C). In addition, cytotoxicity of B7-H3 CAR T cells against sorted PCSCs irradiated at 2Gy/day x 5 days was tested by flow analysis. At E:T ratio of 1:1, PCSCs were almost non-detectable (Fig 6D). This observation was confirmed by the results of the sphere formation assay. Co-culturing FIR-treated PCSCs with B7-H3 CAR T cells (E:T ratio of 1:1) reduced the sphere forming ability 16- and 20-fold for DU145 (p<0.001) and PC3 (p<0.001) cell lines, respectively, compared to FIR-treated PCSCs co-cultured with NT cells (Fig 6E, F).

Targeting FIR-resistant PCSCs with B7-H3 CAR T cells is more effective than either FIR or CAR T cells alone in inhibiting growth of hormone insensitive PCa xenografts in immunodeficient mice.

The demonstrated ability of B7-H3 CAR T cells to eliminate FIR-resistant PCSCs and bulk PCa cells *in vitro* (Fig 6) provided a strong rationale to test if this strategy would be effective in a preclinical PCa xenograft tumor model system using immunodeficient mice bearing DU145 cell line-derived xenografts. The DU145 cell line was derived from a brain metastatic prostate tumor and is hormone insensitive (40), representative of a highly clinically relevant type of PCa (castration-resistant PCa) that is associated with very poor clinical outcomes. FIR was administered over a 5-day period (days 11-15) post-tumor cell inoculation (day 0). B7-H3 CAR T cells were administered on day 15 (Fig 7A), with tumor volumes being monitored biweekly up until day 60. The anti-tumor efficacy (as monitored by tumor volume) of the combination of B7-H3 CAR T cells with FIR was significantly greater than either FIR (p<0.001) or B7-H3 CAR T cells alone (p<0.001) (Fig 7B, H). No treatment-associated toxicity was detected as measured by mouse general health conditions and body weight (Fig 7C). As anticipated, the greater anti-tumor efficacy of B7-H3 CAR T cells and FIR was associated with a decreased percentage of PCSCs in tumors (0.045±0.021%), identified as $ALDH^+CD44^+$ cells, compared to untreated tumors (0.76±0.12%, p<0.05) and tumors treated with FIR+NT cells (1.35±0.13%, p<0.01), as assessed by flow analysis (Fig 7D, E). Although the difference wasn't significant compared

Author Manuscript Author Manuscript Author Manuscript Author Manuscript

to tumors treated with B7-H3 CAR T cells alone (0.22±0.14%, p=0.2257), when PCSCs were defined as sphere forming cells, tumors treated by B7-H3 CAR T cells and FIR displayed a significantly lower percentage PCSCs (2.4±0.89%) compared to untreated tumors (20.2±1.3%, p<0.001), tumors treated with FIR+NT alone (49.2±5.63%, p<0.001), and tumors treated with B7-H3 CAR T cells alone (10.4±1.14%, p<0.001) (Fig 7F, G). It is noteworthy that these *in vivo* data indicate FIR increased PCSCs; this conclusion is in agreement with previous *in vitro* findings of FIR inducing PCSCs (Fig 1). To confirm these data and identify the optimal timing for the combination of FIR and B7-H3 CAR T cells, we tested FIR combined with B7-H3 CAR T cells given at different days post-FIR in immunodeficient NSG mice bearing xenografts derived from PC3, the other castration-resistant PCa cell line used in this study (Fig 8A). We found that the combination of FIR and B7-H3 CAR T cells is more effective than FIR alone at inhibiting growth (as monitored by tumor volume) of hormone insensitive PC3 xenografts regardless of whether B7-H3 CAR T cells were given 1, 3, or 7 days post-FIR (p<0.001) (Fig 8B). However, the anti-tumor effect of the combination was the greatest 3 days post-FIR (FIR(3)+B7-H3 CAR T vs. FIR(1)+B7-H3 CAR T: p<0.01; FIR(3)+B7-H3 CAR T vs. FIR(7)+B7-H3 CAR T: p<0.001). Moreover, CAR T cell administration 1 day post-FIR was more effective than administration 7 days post-FIR (FIR(1)+B7-H3 CAR T vs. FIR(7)+B7-H3 CAR T: p<0.001) (Fig 8B). These data indicate that the duration of FIR-induced B7-H3 upregulation (1-3 days post-FIR) (Supplementary Fig 3A, C) is associated with the optimal time-window of B7-H3 CAR T cell administration post-FIR for the greatest anti-tumor efficacy (Fig 8B). Once again, the anti-tumor efficacy of the combination of FIR and B7-H3 CAR T cells was inversely associated with PCSCs within tumors, measured either as $ALDH^+CD44^+$ cells (Fig 8D, E) or sphere forming cells (Fig 8F, G).

DISCUSSION

Although RT (FIR) is an important therapy for newly diagnosed localized PCa and/or low-volume metastatic PCa, the resistance of PCSCs to radiation can hinder achieving beneficial therapeutic outcomes in many cases (12,36). Therefore, it is critical to develop an effective therapeutic approach to enhance radiation in eradicating PCSCs, the subpopulation of tumor cells that have been shown to be highly resistant to chemotherapy and radiation in many types of human malignancies. PCSCs like other CSCs are considered to be a major cause of treatment failure that ultimately results in recurrence and metastasis (10,12).

The preclinical findings reported here establish the immune checkpoint B7-H3 as an attractive candidate for CAR T cell-based immunotherapy of PCa that is resistant to FIR. The ability to target the immune checkpoint B7-H3 expressed on human PCSCs and bulk PCa cells using B7-H3 CAR T cells was established in a series of experiments. We first demonstrated extensive and higher levels of B7-H3 expression on PCSCs compared to bulk PCa cells using the B7-H3-specfic mAb 376.96 (Fig 3), which was made in our laboratory. scFv 376.96 was used for generation of the B7-H3 CAR T cell construct. Subsequent experiments established the efficient and specific ability of B7-H3 CAR T cells to target B7-$H3^+$ PCSCs and bulk PCa cells and mediate cytolysis of B7-$H3^+$ cells in *in vitro*-based assays. The cytotoxic activity of the CAR T cells was high. All non-irradiated B7-$H3^+$ target cells tested were eliminated at an E:T ratio of 5:1. When tested at a lower E:T ratio, the

Author Manuscript Author Manuscript Author Manuscript Author Manuscript

cytotoxicity of B7-H3 CAR T cells was found to be higher against PCSCs than against bulk PCa cells; the former express higher levels of B7-H3 compared to bulk cells (Fig 6). Most importantly, FIR upregulated B7-H3 expression on PCSCs and bulk PCa tumor cells in both cell lines tested. Enhanced B7-H3 expression by PCSCs was IR dose- and time-dependent (Fig 4). Furthermore, B7-H3 CAR T cells were found to be able to effectively eliminate FIR-resistant PCSCs *in vitro* (E:T ratio of 1:1) and *in vivo* (a single injection of 2×10^6 cells) (Fig 6–8). As a result, the combination of FIR (4Gy/day x 5 days) and B7-H3 CAR T cells was more effective in controlling both DU145- and PC3-derived PCa xenograft growth in NSG mice than FIR or B7-H3 CAR T cells administered as monotherapies (Fig 7, 8). It is noteworthy that the duration of FIR or single-dose irradiation (IR)-induced upregulation of B7-H3 on PCa cells and PCSCs lasts for up to 3 days (Fig 4G–J, Supplementary Fig 3A, C), which is associated with the optimal time-window for B7-H3 CAR T *in vivo* delivery, i.e, 1-3 days post-FIR (although 3 days appeared to be slightly better than 1 day), to achieve its greatest anti-tumor efficacy in the PC3-derived xenograft mouse model (Fig 8).

To our knowledge, this is the first study to demonstrate the potential of targeting the immune checkpoint B7-H3, which is highly expressed on FIR-resistant PCSCs, with a CAR T cell therapy to achieve beneficial outcomes for PCa. The study by Deng et al, aimed at targeting PCSCs expressing EpCAM by EpCAM-specific CAR T cells in xenograft PC3 PCa models, had only modest anti-tumor efficacy compared to treatment with NT cells (41). Combinatorial approaches to cancer treatment involving systemic therapy and RT protocols may be more effective than monotherapies. Attempts have been made to use RT to increase efficacy of CAR T cell therapy for cancer in preclinical and clinical studies. The combination of a single dose of IR (4Gy) with NKG2D CAR T cells in one study and IR (2Gy) with sLeA CAR T cells in another was shown to enhance the cytotoxicity against tumor cells *in vitro* and in murine glioblastoma cells orthotopically grafted in syngeneic immunocompetent mice and in human PDAC cells orthotopically grafted in immunodeficient mice, respectively (42,43). In the glioblastoma study, the mechanisms of synergy between IR and CAR T cells were attributed to increased IFNγ production by tumor-infiltrating CAR T cells and their accumulation within the tumor microenvironment (42), while enhanced sensitivity of the IR-treated PDAC cells to apoptosis appeared to be mediated by TRAIL produced by the tumor-engaged sLeA CAR T cells (43). More importantly, another clinical trial showed that patients with diffuse large B cell lymphoma given RT (40 Gy in 2 Gy/fraction) to debulk tumor burden before infusion of CAR T cells against CD19, CD20, or CD22, had better clinical responses but also experienced only mild cytokine release syndrome (CRS) (grade 1/2) and no neurotoxicity, which are the typical adverse events associated with CAR T therapy, compared to the cohort treated with intensive combined chemotherapy to debulk tumor burden. All the patients in the latter group experienced CAR T cell-related severe CRS (grade 3/4/5) and 57.1% patients experienced neurotoxicity (44). Consistent with these findings are the results of a clinical trial in patients with non-Hodgkin lymphoma who received induction RT on localized tumor burden (range 20-45Gy in 2.2-4.5Gy/fraction given <30 days before infusion of CAR T cells against CD19) and who did not experience serious CRS or neurotoxicity (49).

In agreement with these preclinical and clinical reports, the results of this study not only provides evidence to support B7-H3 CAR T therapy and the need to combine it with RT in

Author Manuscript Author Manuscript Author Manuscript Author Manuscript

PCa, but also offers potential additional advantages as follows i) establishes B7-H3 as an important target for PCa on both PCSCs and PCa, ii) may provide an opportunity to enhance activity of CAR T cells and tumor-infiltrating CTLs by targeting immune checkpoint B7-H3 using CAR T cells, iii) IR could potentiate the effects of CAR T cells by providing a favorable tumor microenvironment and increase density of infiltrating CTLs by upregulation of MHC class I (45,46). Thus, the approach presented in this paper provides a sound basis for further development of this unique combinatorial model of RT and B7-H3 CAR T cell therapy for PCa in a complementary manner for better clinical outcomes.

It is noteworthy that accumulated data from dose escalation studies in the past decades have suggested that high dose IR may improve biochemical-failure survival and/or metastasis-free survival, but dose escalation is limited by presence of adjacent normal tissues/organs and is often associated with increased risks for normal tissue toxicities in PCa patients (47,48). Clearly, results of this study suggest that combination of B7-H3 CAR T cells with RT should be investigated to improve clinical outcomes in localized PCa with high-risk features and/or low volume metastasis. Additionally, it is known that CAR T cell infusion before IR in the clinical setting worked well (44,49). A case study of a refractory myeloma patient in which FIR (20Gy in 4Gy/fraction) was delivered locally, shortly after BCMA-targeted CAR T cell therapy showed a potential synergistic clinical response and T cell clonal expansion (50). Therefore, the sequence of CAR T cell administration in relation to RT, e.g., either before, during or after RT, should be further compared and optimized. Likewise, the dose and frequency of RT in combination with a given CAR T cell therapy must also be tested and optimized in the future to maximize therapeutic ratio, improving efficacy while minimizing toxicity for PCa patients.

Supplementary Material

Refer to Web version on PubMed Central for supplementary material.

Acknowledgments

Financial Support: This work was supported by grants R01CA226981-01A1 (X.W.), W81XWH-16-1-0500 Department of Defense Breakthrough Award Level 2 (S.F.), R03CA223886 (S.F.) and Natural Science Foundation of Jiangxi Province 20202BAB206018 (Y.Z.).

Abbreviations:

ALDH	aldehyde dehydrogenase
BSA	bovine serum albumin
CAR	chimeric antigen receptor
CRS	cytokine release syndrome
CSC	cancer stem cell
CTL	cytotoxic T lymphocyte
E:T	effector to target

Author Manuscript Author Manuscript Author Manuscript Author Manuscript

EpCAM	epithelial cell adhesion molecule
FBS	fetal bovine serum
FIR	fractionated irradiation
Gy	Gray
IR	irradiation
KO	knockout
mAb	monoclonal antibody
MFI	mean fluorescence intensity
NT	non-transduced T
OC	ovarian cancer
PBMC	peripheral blood mononuclear cell
PBS	phosphate-buffered saline
PCa	prostate cancer
PCSC	prostate cancer stem cell
PDAC	pancreatic ductal adenocarincoma
PSCA	prostate stem cell antigen
PSMA	prostate-specific membrane antigen
RT	radiation therapy
scFv	single-chain variable fragment
TA	tumor antigen

REFERENCES

1. American Cancer Society. Cancer Facts & Figures 2020 2020.
2. Punnen S, Cooperberg MR, D'Amico AV, Karakiewicz PI, Moul JW, Scher HI, et al. Management of biochemical recurrence after primary treatment of prostate cancer: a systematic review of the literature. European urology 2013;64:905–15 [PubMed: 23721958]
3. NCCN. NCCN Clinical Practice Guidelines in Oncology (NCCN Guidelines) Prostate Cancer Version 1.2020. 2020
4. Rosenbaum E, Partin A, Eisenberger MA. Biochemical relapse after primary treatment for prostate cancer: studies on natural history and therapeutic considerations. Journal of the National Comprehensive Cancer Network 2004;2:249–56 [PubMed: 19795608]
5. Simmons MN, Stephenson AJ, Klein EA. Natural history of biochemical recurrence after radical prostatectomy: risk assessment for secondary therapy. European urology 2007;51:1175–84 [PubMed: 17240528]
6. Chaiswing L, Weiss HL, Jayswal RD, Clair DKS, Kyprianou N. Profiles of radioresistance mechanisms in prostate cancer. Critical Reviews™ in Oncogenesis 2018;23

Author Manuscript Author Manuscript Author Manuscript Author Manuscript

7. Morgan PB, Hanlon AL, Horwitz EM, Buyyounouski MK, Uzzo RG, Pollack A. Timing of biochemical failure and distant metastatic disease for low, intermediate, and high risk prostate cancer after radiotherapy. Cancer 2007;110:68–80 [PubMed: 17520705]
8. Cong J, Wang Y, Zhang X, Zhang N, Liu L, Soukup K, et al. A novel chemoradiation targeting stem and nonstem pancreatic cancer cells by repurposing disulfiram. Cancer letters 2017;409:9–19 [PubMed: 28864067]
9. Wang Y, Li W, Patel SS, Cong J, Zhang N, Sabbatino F, et al. Blocking the formation of radiation–induced breast cancer stem cells. Oncotarget 2014;5:3743 [PubMed: 25003837]
10. Mei W, Lin X, Kapoor A, Gu Y, Zhao K, Tang D. The contributions of prostate cancer stem cells in prostate cancer initiation and metastasis. Cancers 2019;11:434
11. Ni J, Cozzi P, Hao J, Duan W, Graham P, Kearsley J, et al. Cancer stem cells in prostate cancer chemoresistance. Current cancer drug targets 2014;14:225–40 [PubMed: 24720286]
12. Tsing T, Beretov J, Ni J, Bai X, Bucci J, Graham P, et al. Cancer stem cells in prostate cancer radioresistance. Cancer letters 2019
13. Kantoff PW, Higano CS, Shore ND, Berger ER, Small EJ, Penson DF, et al. Sipuleucel-T immunotherapy for castration-resistant prostate cancer. New England Journal of Medicine 2010;363:411–22
14. Boettcher AN, Usman A, Morgans AK, VanderWeele D, Sosman J, Wu J. Past, current, and future of immunotherapies for prostate cancer. Frontiers in oncology 2019;9:884 [PubMed: 31572678]
15. Du H, Hirabayashi K, Ahn S, Kren NP, Montgomery SA, Wang X, et al. Antitumor responses in the absence of toxicity in solid tumors by targeting B7-H3 via chimeric antigen receptor T cells. Cancer Cell 2019;35:221–37. e8. [PubMed: 30753824]
16. June CH, O'Connor RS, Kawalekar OU, Ghassemi S, Milone MC. CAR T cell immunotherapy for human cancer. Science 2018;359:1361–5 [PubMed: 29567707]
17. Majzner RG, Mackall CL. Tumor antigen escape from CAR T-cell therapy. Cancer discovery 2018;8:1219–26 [PubMed: 30135176]
18. Shah N, Maatman T, Hari PN, Johnson B. Multi targeted CAR-T cell therapies for B-cell malignancies. Frontiers in oncology 2019;9:146 [PubMed: 30915277]
19. Gorchakov AA, Kulemzin SV, Kochneva GV, Taranin AV. Challenges and prospects of chimeric antigen receptor T-cell therapy for metastatic prostate cancer. European Urology 2020;77:299–308 [PubMed: 31471138]
20. Heinrich M- C, Göbel C, Kluth M, Bernreuther C, Sauer C, Schroeder C, et al. PSCA expression is associated with favorable tumor features and reduced PSA recurrence in operated prostate cancer. BMC cancer 2018;18:612 [PubMed: 29855276]
21. Trover JK, Beckett ML, Wright GL Jr. Detection and characterization of the prostate specific membrane antigen (PSMA) in tissue extracts and body fluids. International journal of Cancer 1995;62:552–8 [PubMed: 7665226]
22. Zappasodi R, Merghoub T, Wolchok JD. Emerging concepts for immune checkpoint blockade-based combination therapies. Cancer cell 2018;33:581–98 [PubMed: 29634946]
23. Benzon B, Zhao S, Haffner M, Takhar M, Erho N, Yousefi K, et al. Correlation of B7-H3 with androgen receptor, immune pathways and poor outcome in prostate cancer: an expression-based analysis. Prostate cancer and prostatic diseases 2017;20:28–35 [PubMed: 27801901]
24. Chavin G, Sheinin Y, Crispen PL, Boorjian SA, Roth TJ, Rangel L, et al. Expression of immunosuppresive B7-H3 ligand by hormone-treated prostate cancer tumors and metastases. Clinical Cancer Research 2009;15:2174–80 [PubMed: 19276267]
25. Powderly J, Cote G, Flaherty K, Szmulewitz R, Ribas A, Weber J. Interim results of an ongoing phase 1, dose escalation study of MGA271 (Enoblituzumab), an Fc-optimized humanized anti-B7-H3 monoclonal antibody, in patients with advanced solid cancer. J Immuno Ther Cancer 2015;3:8
26. Kontos F, Michelakos T, Kurokawa T, Sadagopan A, Schwab JH, Ferrone CR, et al. B7-H3: an attractive target for antibody-based immunotherapy. Clin Cancer Res. 2020
27. Suh W- K, Gajewska BU, Okada H, Gronski MA, Bertram EM, Dawicki W, et al. The B7 family member B7-H3 preferentially down-regulates T helper type 1–mediated immune responses. Nature immunology 2003;4:899–906 [PubMed: 12925852]

Author Manuscript Author Manuscript Author Manuscript Author Manuscript

28. Ma J, Ma P, Zhao C, Xue X, Han H, Liu C, et al. B7-H3 as a promising target for cytotoxicity T cell in human cancer therapy. Oncotarget 2016;7:29480 [PubMed: 27121051]
29. Fizazi K, Tran N, Fein L, Matsubara N, Rodriguez-Antolin A, Alekseev BY, et al. Abiraterone plus prednisone in metastatic, castration-sensitive prostate cancer. New England Journal of Medicine 2017;377:352–60
30. Parker CC, James ND, Brawley CD, Clarke NW, Hoyle AP, Ali A, et al. Radiotherapy to the primary tumour for newly diagnosed, metastatic prostate cancer (STAMPEDE): a randomised controlled phase 3 trial. The Lancet 2018;392:2353–66
31. Sweeney CJ, Chen Y- H, Carducci M, Liu G, Jarrard DF, Eisenberger M, et al. Chemohormonal therapy in metastatic hormone-sensitive prostate cancer. New England Journal of Medicine 2015;373:737–46
32. Sun T, Yang W, Toprani SM, Guo W, He L, DeLeo AB, et al. Induction of immunogenic cell death in radiation-resistant breast cancer stem cells by repurposing anti-alcoholism drug disulfiram. Cell Communication and Signaling 2020;18:1–14 [PubMed: 31900175]
33. Kasten BB, Gangrade A, Kim H, Fan J, Ferrone S, Ferrone CR, et al. 212Pb-labeled B7-H3-targeting antibody for pancreatic cancer therapy in mouse models. Nuclear medicine and biology 2018;58:67–73 [PubMed: 29413459]
34. Zhou R, Yazdanifar M, Roy LD, Whilding LM, Gavrill A, Maher J, et al. CAR T cells targeting the tumor MUC1 glycoprotein reduce triple-negative breast cancer growth. Frontiers in immunology 2019;10:1149 [PubMed: 31178870]
35. Morgan SC, Hoffman K, Loblaw DA, Buyyounouski MK, Patton C, Barocas D, et al. Hypofractionated radiation therapy for localized prostate cancer: Executive summary of an ASTRO, ASCO, and AUA evidence-based guideline. Practical radiation oncology 2018;8:354–60 [PubMed: 30322661]
36. Saga R, Matsuya Y, Takahashi R, Hasegawa K, Date H, Hosokawa Y. Analysis of the high-dose-range radioresistance of prostate cancer cells, including cancer stem cells, based on a stochastic model. Journal of radiation research 2019;60:298–307 [PubMed: 31034058]
37. Wang X, Ma Z, Xiao Z, Liu H, Dou Z, Feng X, et al. Chk1 knockdown confers radiosensitization in prostate cancer stem cells. Oncology reports 2012;28:2247–54 [PubMed: 23027394]
38. Chang L, Graham P, Hao J, Ni J, Bucci J, Cozzi P, et al. Acquisition of epithelial– mesenchymal transition and cancer stem cell phenotypes is associated with activation of the PI3K/Akt/mTOR pathway in prostate cancer radioresistance. Cell death & disease 2013;4:e875–e [PubMed: 24157869]
39. Yu C, Yao Z, Jiang Y, Keller ET. Prostate cancer stem cell biology. Minerva urologica e nefrologica 2012;64:19 [PubMed: 22402315]
40. Ciardiello C, Leone A, Lanuti P, Roca MS, Moccia T, Minciacchi VR, et al. Large oncosomes overexpressing integrin alpha-V promote prostate cancer adhesion and invasion via AKT activation. Journal of Experimental and Clinical Cancer Research 2019:38:317 [PubMed: 31319863]
41. Deng Z, Wu Y, Ma W, Zhang S, Zhang Y-Q. Adoptive T-cell therapy of prostate cancer targeting the cancer stem cell antigen EpCAM. BMC immunology 2015;16:1 [PubMed: 25636521]
42. Weiss T, Weller M, Guckenberger M, Sentman CL, Roth P. NKG2D-based CAR T cells and radiotherapy exert synergistic efficacy in glioblastoma. Cancer research 2018;78:1031–43 [PubMed: 29222400]
43. DeSelm C, Palomba ML, Yahalom J, Hamieh M, Eyquem J, Rajasekhar VK, et al. Low-dose radiation conditioning enables CAR T cells to mitigate antigen escape. Molecular Therapy 2018;26:2542–52 [PubMed: 30415658]
44. Qu C, Ping N, Kang L, Liu H, Qin S, Wu Q, et al. Radiation Priming Chimeric Antigen Receptor T-Cell Therapy in Relapsed/Refractory Diffuse Large B-Cell Lymphoma With High Tumor Burden. Journal of Immunotherapy 2020;43:32–7 [PubMed: 31219975]
45. Minn I, Rowe SP, Pomper MG. Enhancing CAR T-cell therapy through cellular imaging and radiotherapy. The Lancet Oncology 2019;20:e443–e51 [PubMed: 31364596]
46. Reits EA, Hodge JW, Herberts CA, Groothuis TA, Chakraborty M, K. Wansley E, et al. Radiation modulates the peptide repertoire, enhances MHC class I expression, and induces successful

Author Manuscript Author Manuscript Author Manuscript Author Manuscript

antitumor immunotherapy. The Journal of experimental medicine 2006;203:1259–71 [PubMed: 16636135]

47. Lardas M, Liew M, van den Bergh RC, De Santis M, Bellmunt J, Van den Broeck T, et al. Quality of life outcomes after primary treatment for clinically localised prostate cancer: a systematic review. European urology 2017;72:869–85 [PubMed: 28757301]
48. Wallis CJ, Glaser A, Hu JC, Huland H, Lawrentschuk N, Moon D, et al. Survival and complications following surgery and radiation for localized prostate cancer: an international collaborative review. European urology 2018;73:11–20 [PubMed: 28610779]
49. Wright CM, LaRiviere MJ, Baron JA, Uche C, Xiao Y, Arscott WT, et al. Bridging Radiation Therapy Before Commercial Chimeric Antigen Receptor T-Cell Therapy for Relapsed or Refractory Aggressive B-Cell Lymphoma. International Journal of Radiation Oncology, Biology, Physics 2020:108:178–88
50. Smith EL, Mailankody S, Staehr M, Wang X, Senechal B, Purdon TJ, et al. BCMA-targeted CAR T-cell therapy plus radiotherapy for the treatment of refractory myeloma reveals potential synergy. Cancer immunology research 2019

Author Manuscript Author Manuscript Author Manuscript Author Manuscript

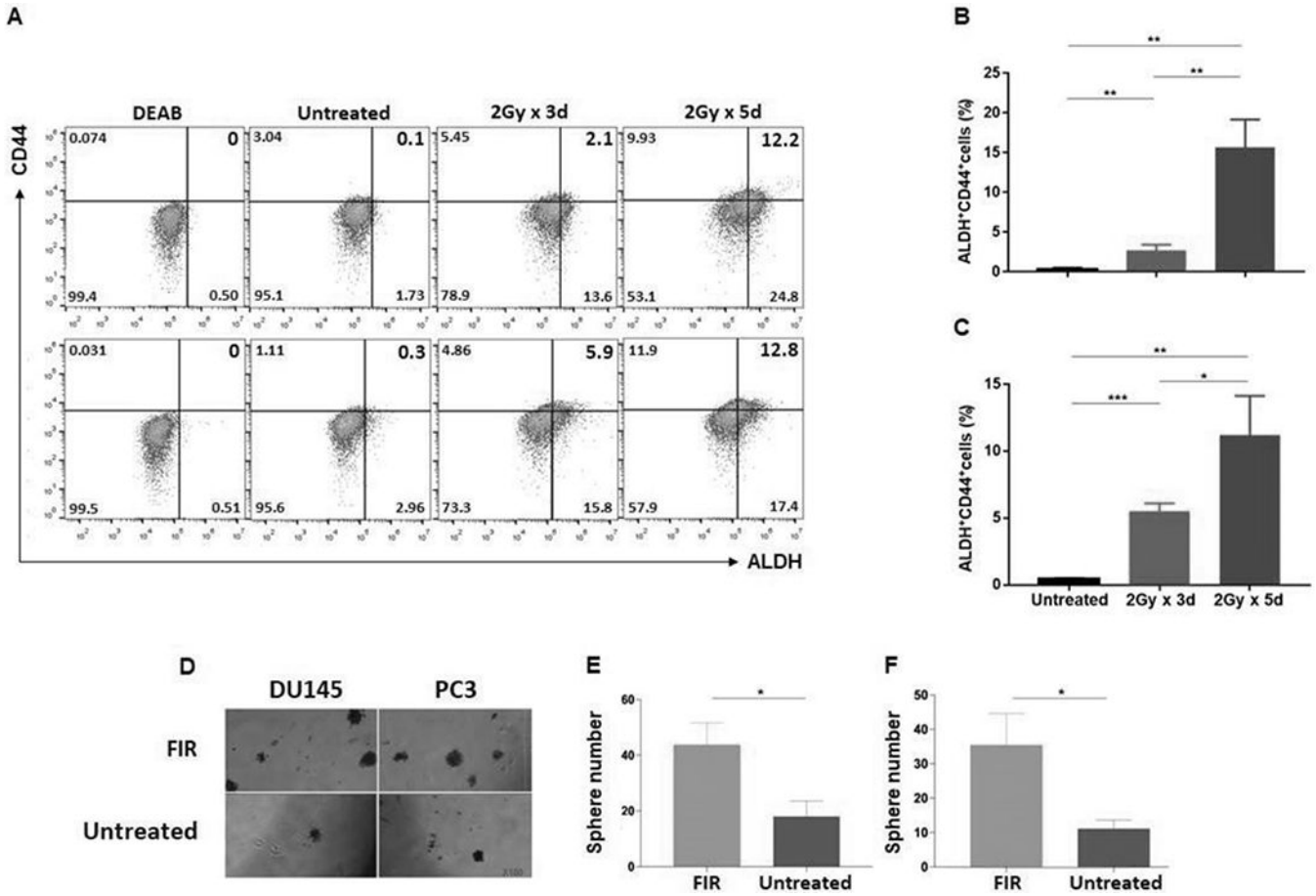

Figure 1. PCSCs are FIR-resistant.

PCa cells were irradiated at doses and times as indicated, and after 24hrs analyzed for $ALDH^+CD44^+$ cells by flow cytometry. Data are shown for DU145 (**A: top**) and PC3 (**A: bottom**) cell lines. $ALDH^+CD44^+$ PCSCs (%) are presented in the upper right quadrant. DEAB, an inhibitor of ALDH1/3 isoforms, was used to establish the baseline fluorescence as the gating reference standard of $ALDH^-$ population. Mean± SD of $ALDH^+CD44^+$ cells (%) are shown for cell lines DU145 (**B**) and PC3 (**C**). Cells plated in 6-well cell culture plates (Corning) at a density of 5×10^5 cells/well in 2 mL RPMI 1640 medium containing 10% FBS were treated with FIR (2Gy/day x 5 days). Cells were trypan blue stained to exclude dead cells and living cells were tested for their ability to form spheres. After 7-10 days, small spheres were detected by microscopy. At day 18, spheres/well were counted. Representative photographs of DU145 and PC3 cells lines are shown (100x) (**D**) as well as mean ± SD of spheres/well for DU145 (**E**) and PC3 (**F**). The experiments were repeated 3 times. *p<0.05; **<0.01; ***<0.001.

Author Manuscript
Author Manuscript
Author Manuscript
Author Manuscript

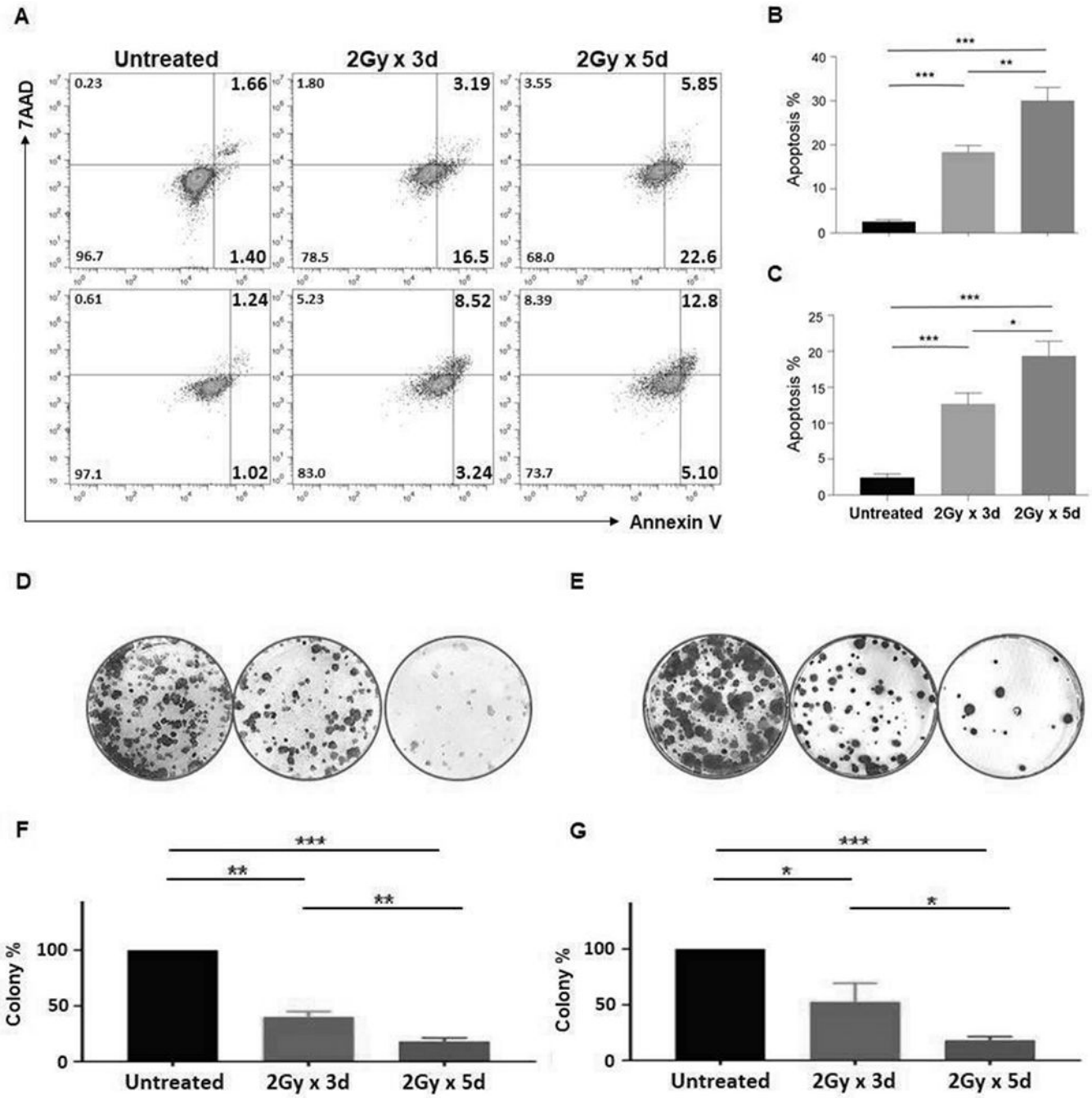

Figure 2. PCa cells are resistant to FIR-induced apoptosis.

PCa cells were irradiated at doses and times as indicated, and 24hrs later were assessed for apoptosis using Annexin V/7-AAD staining. Data for DU145 (**A:top**) and PC3 (**A:bottom**) cell lines are shown. Annexin^{+} apoptotic cells (%) are presented in the right quadrants. Mean ± SD of apoptotic cells (including 7AAD+ late apoptotic or necrotic cells) (%) are shown for DU145 (**B**) and PC3 (**C**) cell lines. The irradiated cells were trypan blue stained to exclude dead cells, and living cells were tested for their ability to form colonies. At day 12, colonies/well were counted. The colonies in untreated wells were too numerous and set as 100%.

Author Manuscript Author Manuscript Author Manuscript Author Manuscript

Representative pictures of DU145 (**D**) and PC3 (**E**) and mean ± SD of colonies (%) for DU145 (**F**) and PC3 (**G**) are shown. The experiments were repeated 3 times. *p<0.05; **<0.01; ***<0.001.

Author Manuscript Author Manuscript Author Manuscript Author Manuscript

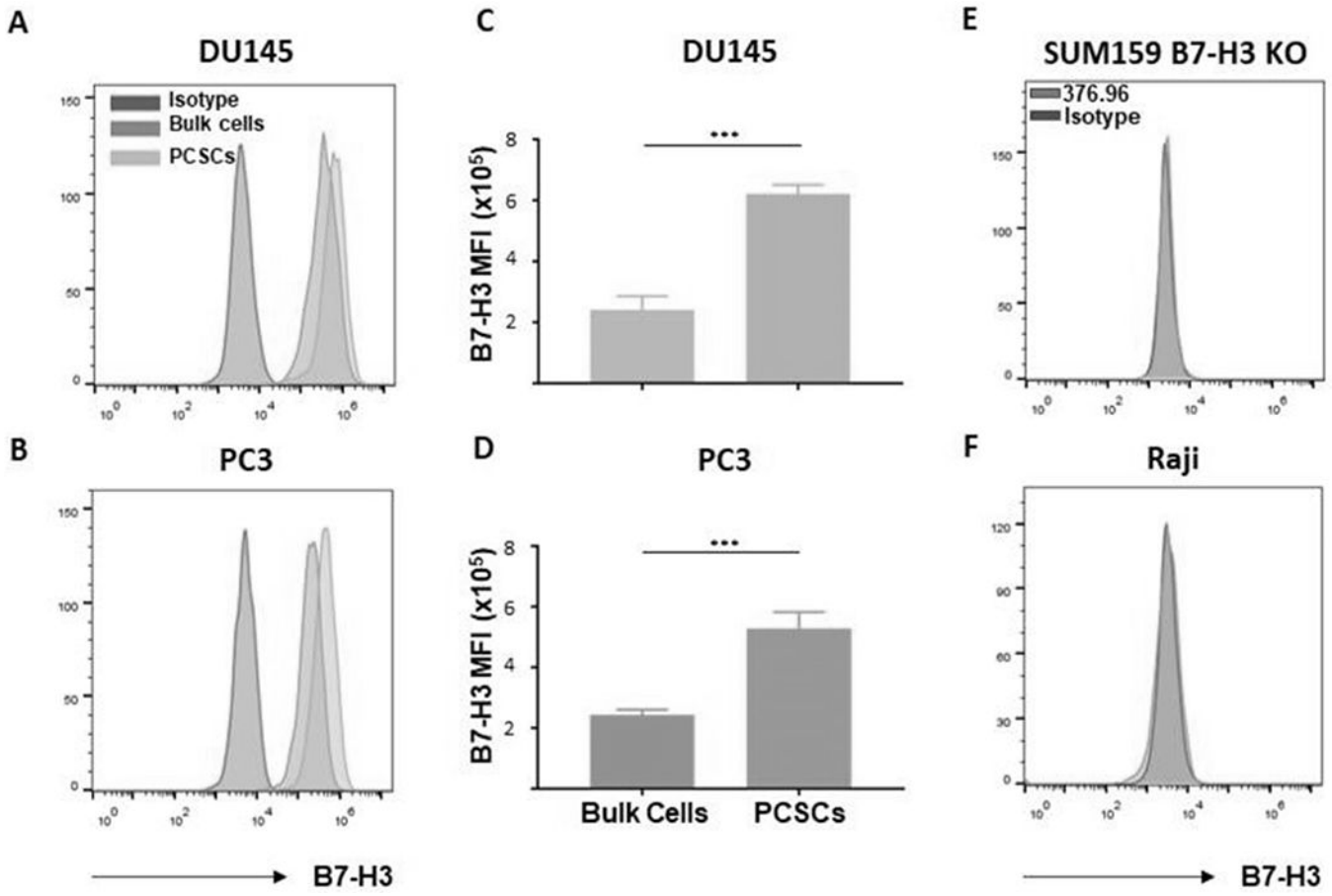

Figure 3. PCSCs express higher levels of B7-H3 antigen than bulk PCa cells.

Sorted ALDH^{+}CD44^{+} PCSCs and unsorted bulk cells were stained with B7-H3-specific mAb 376.96 for detection of B7-H3 expression. Flow cytometry histograms of B7-H3^{+} PCSCs and bulk cells are shown for DU145 (**A**) and PC3 (**B**) cell lines, as well as mean ± SD of B7-H3 MFI for DU145 (**C**) and PC3 (**D**) cell lines. A mouse IgG2a mAb F3C25 was used as the isotype control. The B7-H3^{-} SUM159 B7-H3 KO (**E**) and Raji (**F**) cell lines were used as negative controls. The experiments were repeated 3 times. ***p<0.001.

Author Manuscript Author Manuscript Author Manuscript Author Manuscript

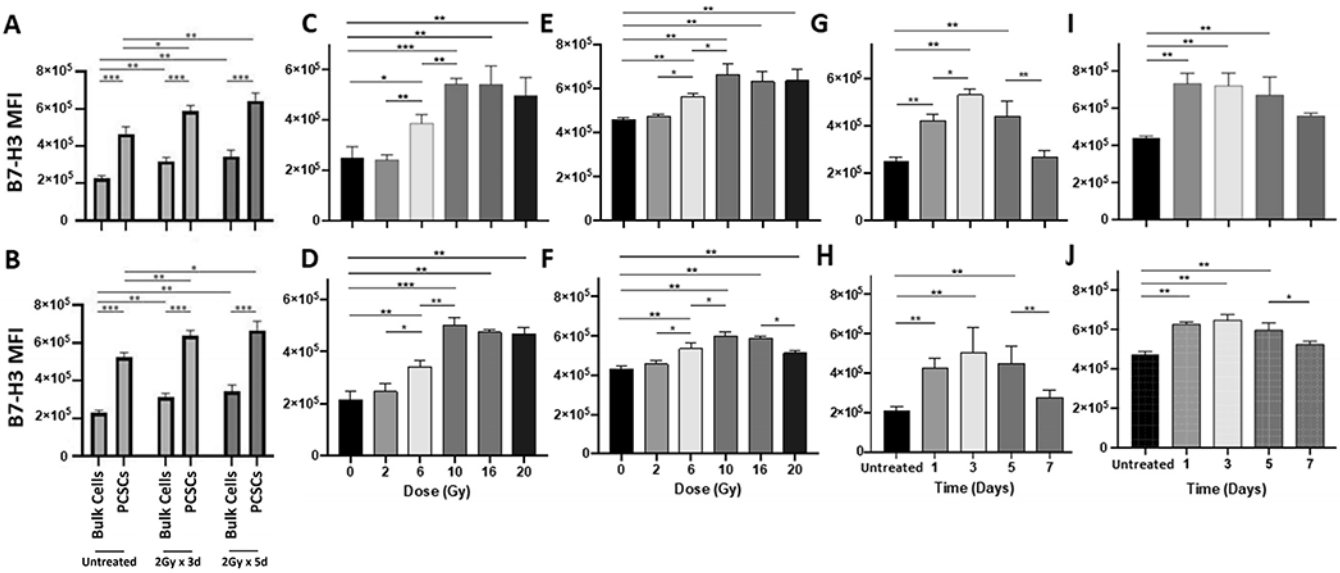

Figure 4. FIR or IR upregulates B7-H3 expression on PCSCs and bulk PCa cells.

Sorted ALDH^{+}CD44^{+} PCSCs and unsorted bulk tumor cells were treated with FIR at doses and times indicated and 24hrs later, the irradiated and non-irradiated (untreated) cells were stained for B7-H3 cell surface expression with B7-H3-specific mAb 376.96. Flow cytometry analysis of B7-H3^{+} bulk tumor cells and PCSCs under each indicated treatment condition were performed. Histograms of flow analysis are shown in Supplementary Fig 1 and mean ± SD of B7-H3 MFI are shown for DU145 (**A**) and PC3 cells (**B**). A single variable dose of IR (0-20Gy) was given to PCa bulk cells or PCSCs and 24 hrs later, B7-H3 expression was detected by flow cytometry analysis. Histograms of flow analysis are shown in Supplementary Fig 2 and mean ± SD of B7-H3 MFI for DU145 bulk cells (**C**) and PCSCs (**E**) and PC3 bulk cells (**D**) and PCSCs (**F**) are shown. A single dose of IR (10Gy) was given to PCa bulk cells or PCSCs, B7-H3 expression was detected at the indicated time points. The histograms of flow analysis are shown in Supplementary Fig 2 and mean ± SD of B7-H3 MFI for DU145 bulk cells (**G**) and PCSCs (**I**) and PC3 bulk cells (**H**) and PCSCs (**J**) are shown. The experiments were repeated 3 times. *p<0.05; **<0.01; ***<0.001.

Author Manuscript Author Manuscript Author Manuscript Author Manuscript

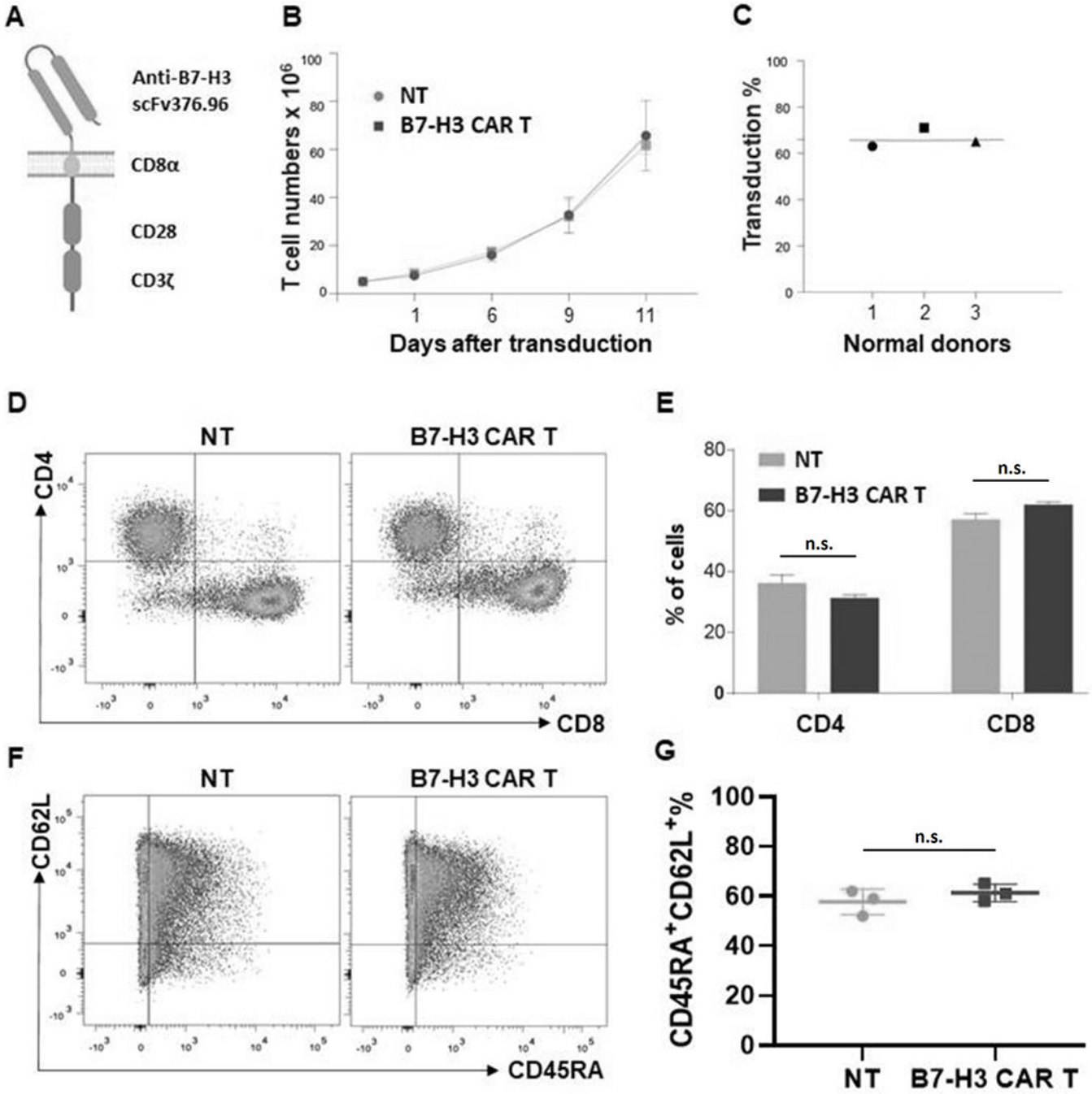

Figure 5. Generation and phenotype of B7-H3 CAR T cells.

Schematic illustration of the B7-H3 CAR construct consisting of anti-human B7-H3 scFv 376.96, CD28 costimulatory domain, and CD3ζ signaling domain (**A**). The time course of the number of expanded transduced and NT cells (**B**), as well as the percentage of B7-H3 CAR T cells out of the total $CD3^+$ cells on day 8 in transduced T cells expanded from 3 individual donors are shown (**C**). Flow cytometry analysis of B7-H3 CAR T cells and NT cells for $CD4^+$ and $CD8^+$ T cells (**D**) and mean ± SD (%) of $CD4^+$ and $CD8^+$ CAR T cells are shown (**E**), in addition to the flow cytometry analysis for $CD45RA^+CD62L^+$ memory-

CAR T cells (**F**) and mean ± SD (%) $CD45RA^{+}CD62L^{+}$ CAR T cells (**G**) are shown. n.s., not significant.

Author Manuscript Author Manuscript Author Manuscript Author Manuscript

Author Manuscript Author Manuscript Author Manuscript Author Manuscript

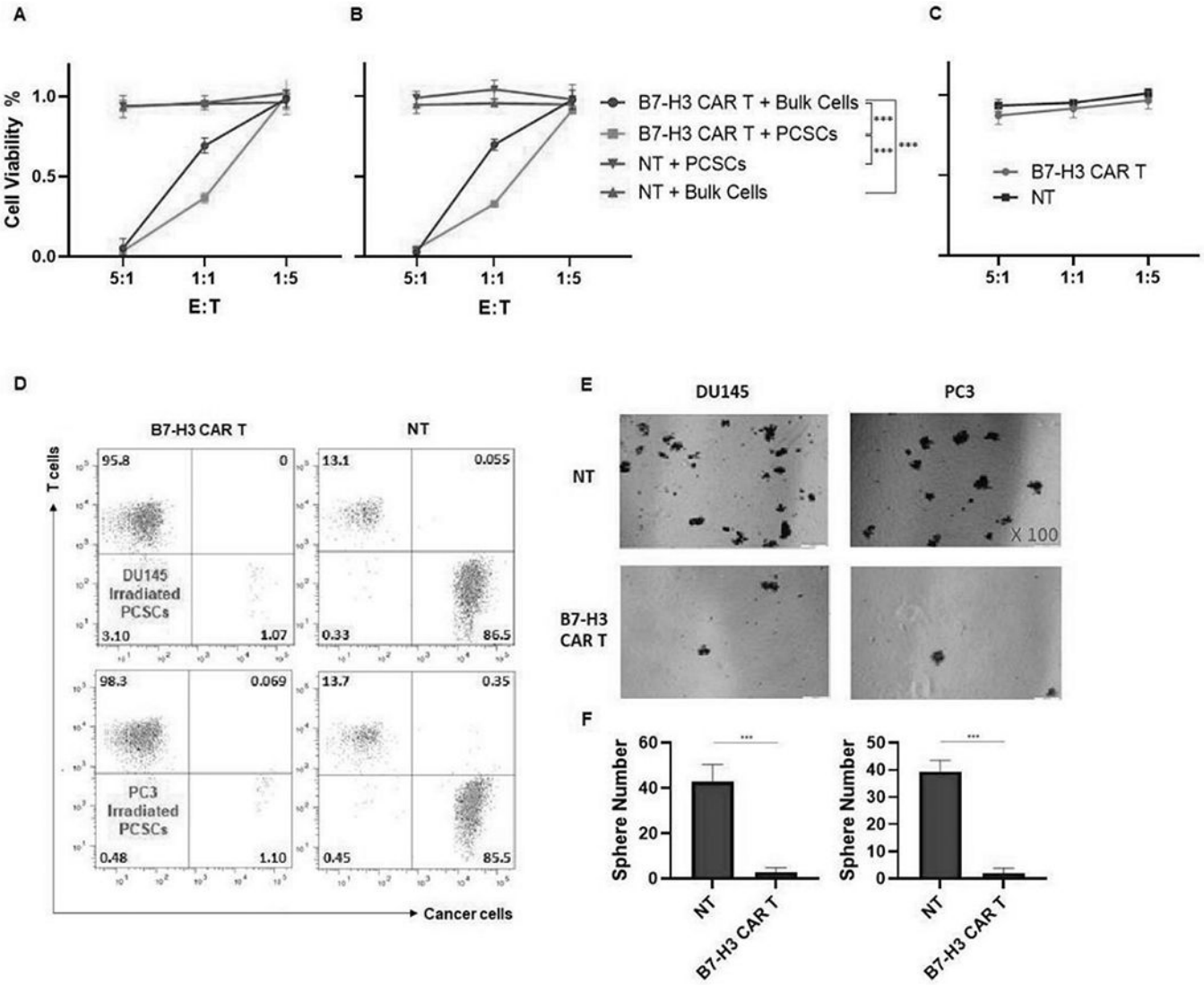

Figure 6. PCSCs are more sensitive to B7-H3 CAR T cells than bulk PCa cells *in vitro*.

B7-H3 CAR T cells and sorted ALDH$^+$CD44$^+$ PCSCs or unsorted bulk PCa target cells were co-cultured at indicated E:T ratios for 48 hrs. CAR T cells in the cell suspension were removed, and the viability of adherent target cells was quantitated by MTT assays. The viability of different cell populations in the cell line DU145 (**A**), PC3 (**B**), and SUM159 B7-H3 KO cells (**C**) are shown. Separately, FIR treated and untreated ALDH$^+$CD44$^+$ PCSCs target cells were co-cultured with B7-H3 CAR T cells at E:T ratio of 1:1 for 48 hrs. The co-cultured cells were analyzed for CD3$^+$ CAR T cells (T cells) and B7-H3$^+$ residual PCSCs (cancer cells) (**D**), and sphere formation ability of the residual PCSCs (100x) (**E**). NT or B7-H3 CAR T cells were co-cultured with FIR treated PCSCs at E:T ratio of 1:1 for 24 hours. Then, the cells were trypan blue stained to exclude dead cells, and living cells were tested for their ability to form spheres. After 7-10 days, small spheres were detected by microscopy. At day 18, spheres/well were counted. Mean ± SD of spheres/well for DU145 (**F: left**) and PC3 (**F: right**) is also shown. NT cells were used as negative controls in these

experiments. FIR dosage used was 2Gy/day for 5 days. The experiments were repeated 3 times. ***p<0.001.

Author Manuscript Author Manuscript Author Manuscript Author Manuscript

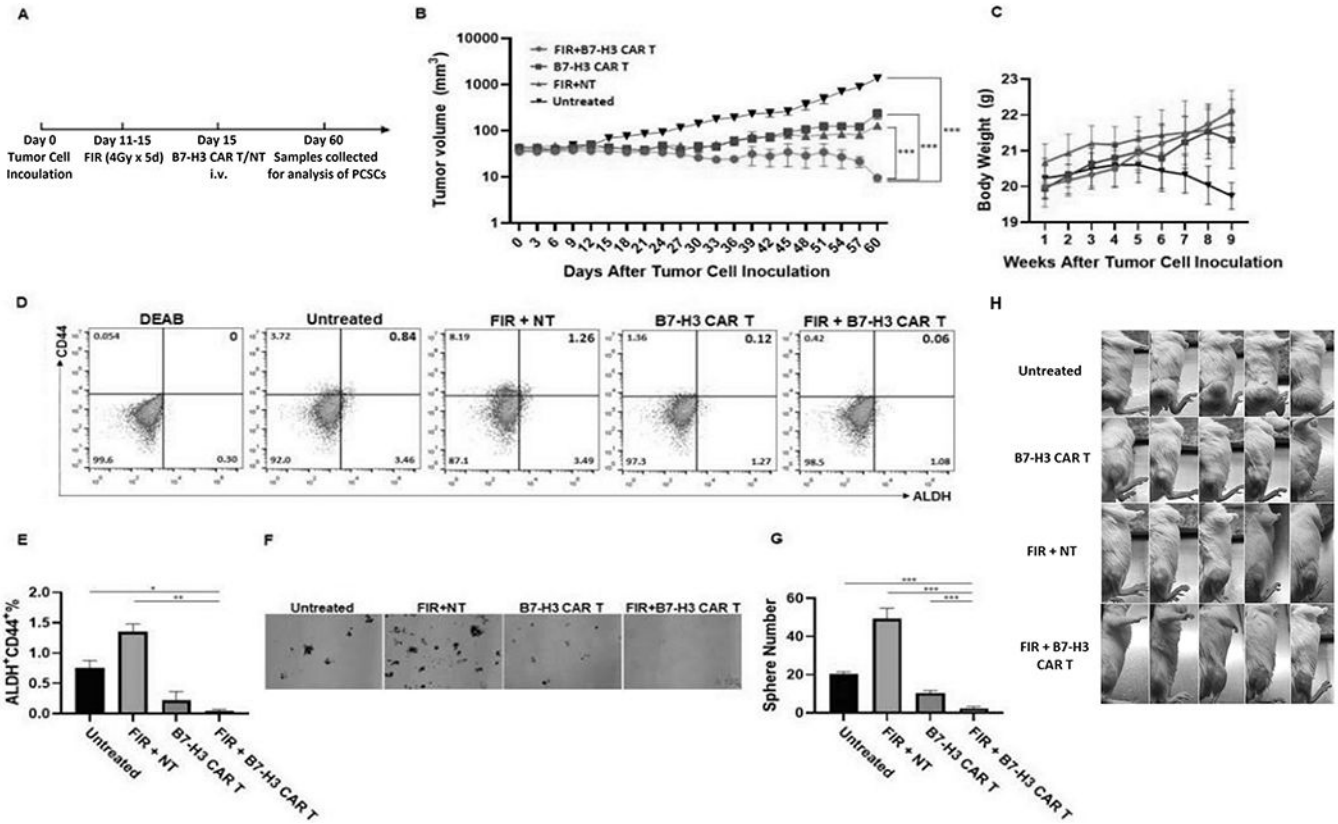

Figure 7. FIR and B7-H3 CAR T cell combinatorial therapy is more effective than either FIR or B7-H3 CAR T cells alone in inhibiting growth of a hormone insensitive DU145 PCa xenograft model.

Schematic diagram of the experimental schedule (**A**), mean ± SEM of tumor volume (**B**) and body weight (**C**) are shown. At the time of sacrifice, the tumor from each mouse was collected. A single cell suspension from 2 pooled tissue samples (tumors from 5 mice of the same group were pooled into 2 pools: one pool consists of 2 and the other pool consists of 3 tissue samples) from each group was assessed by flow cytometry for $ALDH^+CD44^+$ PCSCs (**D**) and mean ± SD (%) of $ALDH^+CD44^+$ PCSCs is shown (**E**). Pools were also analyzed for sphere formation. Shown are representative photographs (x100) (**F**) and mean ± SD of spheres/well (**G**). Photos of tumor-bearing mice are also shown (**H**). *p <0.05; **<0.01; ***<0.001.

Author Manuscript Author Manuscript Author Manuscript Author Manuscript

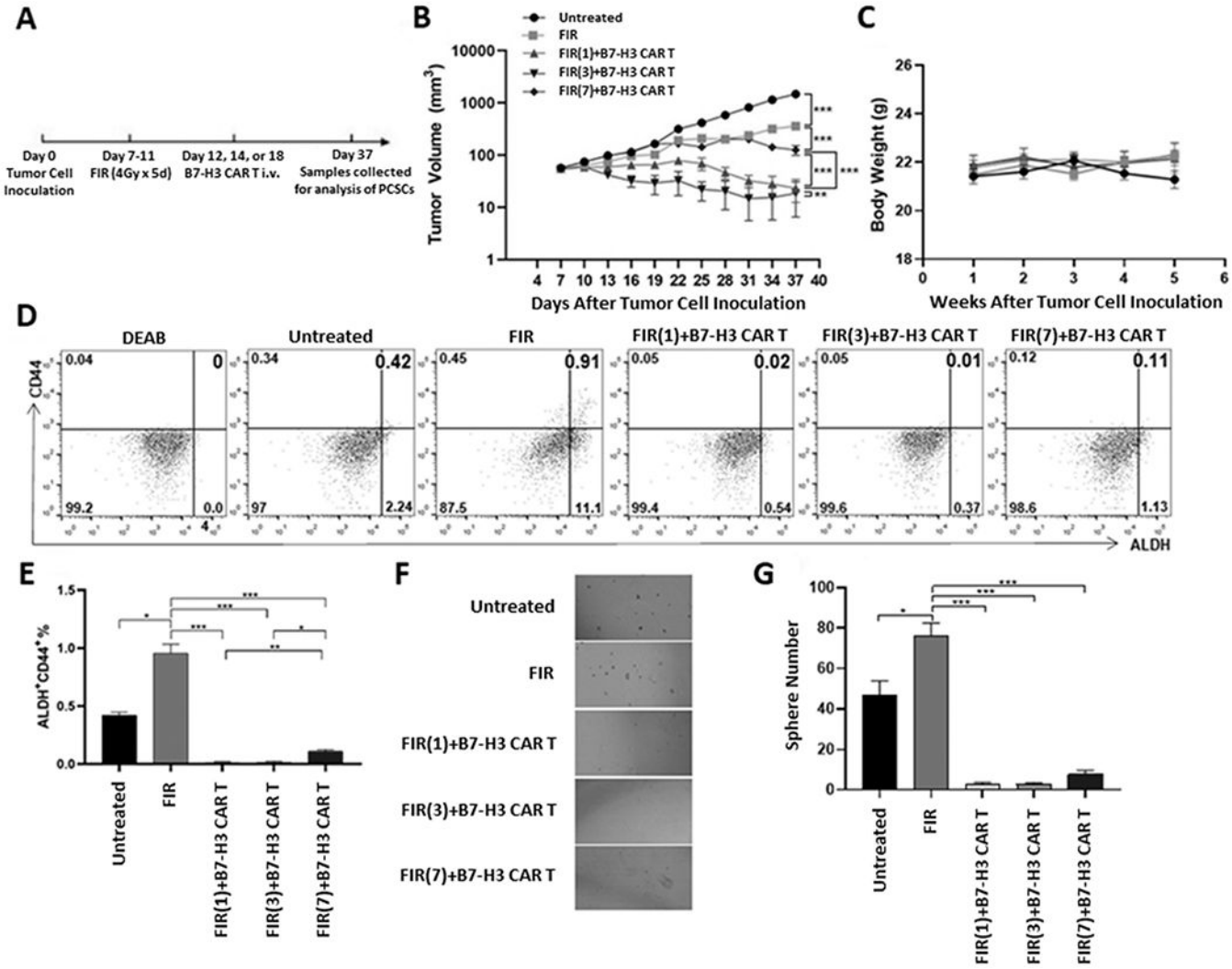

Figure 8. Efficacy of FIR and B7-H3 CAR T cell combinatorial therapy in inhibiting growth of a hormone insensitive PC3 PCa xenograft model is optimal when B7-H3 CAR T cells are administered 1-3 days post-FIR.

Schematic diagram of the experimental schedule (**A**), mean ± SEM of tumor volume (**B**) and body weight (**C**) are shown. At the time of sacrifice, the tumor from each mouse was collected. A single cell suspension from 2 pooled tissue samples (tumors from 5 mice of the same group were pooled into 2 pools: one pool consists of 2 and the other pool consists of 3 tissue samples) from each group was assessed by flow cytometry for $ALDH^{+}CD44^{+}$ PCSCs (**D**) and mean ± SD (%) of $ALDH^{+}CD44^{+}$ PCSCs is shown (**E**). Pools were also analyzed for sphere formation. Shown are representative photographs (x100) (**F**) and mean ± SD of spheres/well (**G**). *p <0.05; **<0.01; ***<0.001.

Author Manuscript Author Manuscript Author Manuscript Author Manuscript